Eddy Viscosity Transport Equations and Their Relation to the k-ϵ Model

F. R. Menter[1]
Head, Development Department,
AEA Technology GmbH,
Staudenfeldweg, 83624 Otterfing, Germany

A formalism will be presented which allows transforming two-equation eddy viscosity turbulence models into one-equation models. The transformation is based on Bradshaw's assumption that the turbulent shear stress is proportional to the turbulent kinetic energy. This assumption is supported by experimental evidence for a large number of boundary layer flows and has led to improved predictions when incorporated into two-equation models of turbulence. Based on it, a new one-equation turbulence model will be derived from the k-ϵ model. The model will be tested against the one-equation model of Baldwin and Barth, which is also derived from the k-ϵ model (plus additional assumptions) and against its parent two-equation model. It will be shown that the assumptions involved in the derivation of the Baldwin-Barth model cause significant problems at the edge of a turbulent layer.

Introduction

Historically, the turbulence models of choice in aerodynamics have been algebraic models, Baldwin and Lomax (1978), Johnson and King (1985), or, to a lesser extent, two-equation eddy viscosity models, like the k-ϵ (Launder and Sharma, 1974) or the k-ω model (Wilcox, 1993). Recently, the monopoly of these models has been challenged by the re-emergence of one-equation turbulence models. While one-equation models have been used earlier (Wilcox, 1993, Bradshaw et al., 1967), most of these older models solve an equation for the turbulent kinetic energy (or the turbulent shear stress), but, like the algebraic models, depend on the specification of an algebraic length-scale in order to calculate the eddy viscosity (see, however, Nee and Kovasznay, 1969 and Gulyaev et al., 1993). The model introduced by Baldwin and Barth (Baldwin and Barth, 1990) solves one transport equation for the eddy viscosity and is independent of an algebraic length-scale which made it very attractive from a numerical point of view. The Baldwin-Barth model was derived from the k-ϵ model and a number of additional simplifying assumptions. However, in the course of the transformation, several diffusive terms were neglected. The effect of changing these terms could not easily be apprehended, and it turns out that the Baldwin-Barth model does perform very differently from the underlying k-ϵ model even for simple equilibrium flows.

The change in the diffusive terms also changes the behavior of the model near the edge of shear layers and renders the equations ill-conditioned in that region as will be shown later. This is a severe issue, as the model was on its way to becoming the favored choice for aerodynamic applications.

The aim of the present effort is to establish a firm connection between one- and two-equation turbulence models. To achieve this goal, the k-ϵ model will be transformed to a one-equation model based on a set of clearly defined assumptions. Numerical results based on the new model will be compared to those of the underlying k-ϵ model and the Baldwin-Barth model. The computations will show that the new one-equation model performs very similar to the k-ϵ model in situations were the underlying assumptions are acceptable. It will also be shown that the Baldwin-Barth model gives results very different from its parent k-ϵ model.

It should be emphasized that the purpose of the present work is to establish a clear connection between one- and two-equation models of turbulence and not to endorse a new model for general use. Due to the close relation to the standard k-ϵ model, the new model inherits some of that model's deficiencies. Especially for aerodynamic flows, the model does not perform as well as models specifically designed for these applications, as the one-equation model of Spalart and Allmaras (Spalart and Allmaras, 1990; Menter, 1994a) or the author's SST k-ω model (Menter, 1993; Menter, 1994b; Menter and Rumsey, 1994). In Menter (1994a) results are shown for the SST and the Spalart-Allmaras model for the same test cases used in the present work. The interested reader can perform a one-to-one comparison between the models.

Turbulence Models

Transformation of the k-ϵ Model. This section will present a transformation of the high Reynolds number version of the k-ϵ model to a one-equation model. For simplicity the equations will be written in boundary layer coordinates—the general form of the equations will be given later. The k-ϵ model reads in boundary layer coordinates (x-streamwise coordinate, y normal to layer, and $D/Dt = \partial/\partial t + u_j(\partial/\partial x_j)$):

$$\frac{Dk}{Dt} = \tilde{\nu}_t\left(\frac{\partial u}{\partial y}\right)^2 - \epsilon + \frac{\partial}{\partial y}\left(\frac{\tilde{\nu}_t}{\sigma_k}\frac{\partial}{\partial y}(k)\right)$$

$$\frac{D\epsilon}{Dt} = c_{\epsilon 1}\frac{\epsilon}{k}\tilde{\nu}_t\left(\frac{\partial u}{\partial y}\right)^2 - c_{\epsilon 2}\frac{\epsilon^2}{k} + \frac{\partial}{\partial y}\left(\frac{\tilde{\nu}_t}{\sigma_\epsilon}\frac{\partial}{\partial y}(\epsilon)\right) \quad (1)$$

with the following definition of the eddy viscosity:

$$\tilde{\nu}_t = c_\mu\frac{k^2}{\epsilon} \quad (2)$$

In order to arrive at a one-equation model, we follow Baldwin and Barth and express the time derivative of the eddy viscosity by the time derivatives of k and ϵ:

$$\frac{D\tilde{\nu}_t}{Dt} = c_\mu\left(2\frac{k}{\epsilon}\frac{Dk}{Dt} - \frac{k^2}{\epsilon^2}\frac{D\epsilon}{Dt}\right) \quad (3)$$

[1] Formerly NASA Ames Research Center.

Contributed by the Fluids Engineering Division for publication in the JOURNAL OF FLUIDS ENGINEERING. Manuscript received by the Fluids Engineering Division December 18, 1996; revised manuscript received July 8, 1997. Associate Technical Editor: M. M. Sindir.

Replacing the total derivatives of k and ϵ on the right-hand side by the right-hand sides of Eq. (1) gives a single transport equation for the eddy viscosity, which, however, depends on k and ϵ as well as on the eddy viscosity:

$$\frac{D\tilde{\nu}_t}{Dt} = F(\tilde{\nu}_t; k; \epsilon) \tag{4}$$

This presents a closure problem with one equation for three unknowns. In order to close the equation, two additional relations have to be provided. The first one is the definition of the eddy viscosity, Eq. (2), which allows one to replace ϵ by the eddy viscosity and the turbulent kinetic energy:

$$\epsilon = c_\mu \frac{k^2}{\tilde{\nu}_t} \tag{5}$$

with $c_\mu = 0.09$. Note that this relation does not involve any additional assumptions and the resulting equation is still equivalent to the original k-ϵ model. A second relation is needed to eliminate k from the right-hand side of Eq. (4) and this relation cannot be derived from the k-ϵ model (otherwise the k-ϵ equations would be overspecified). However, there is a relation readily available that relates the turbulent kinetic energy and the eddy viscosity, which has been confirmed for a large number of experimental boundary layer data and was used by Bradshaw et al. (1967) in the derivation of their one-equation model, namely (see also Townsend, 1962):

$$|-\overline{u'v'}| = \tilde{\nu}_t \left|\frac{\partial u}{\partial y}\right| = a_1 k \tag{6}$$

where a_1 is a constant and $|-\overline{u'v'}|$ is the turbulent shear stress. Note that the relation between the turbulent shear stress and the turbulent kinetic energy that results from standard two-equation models is:

$$|-\overline{u'v'}| = \sqrt{\frac{\text{Production}_k}{\text{Dissipation}_k}}\, a_1 k \tag{7}$$

using $a_1 = \sqrt{c_\mu}$. However, Eq. (7) is not confirmed by experimental evidence in strong adverse pressure gradient flows. It is therefore to be expected that the introduction of Eq. (6) will actually lead to improved predictions of non-equilibrium flows.

Since we have a complete set of equations, the one-equation model can be derived by straightforward substitution. The result is:

$$\begin{aligned}\frac{D\tilde{\nu}_t}{Dt} = {} & c_1\tilde{\nu}_t\left|\frac{\partial u}{\partial y}\right| - c_2\tilde{\nu}_t^2\left(\frac{\dfrac{\partial}{\partial y}\left|\dfrac{\partial u}{\partial y}\right|}{\left|\dfrac{\partial u}{\partial y}\right|}\right)^2 + \frac{\partial}{\partial y}\left(\frac{\tilde{\nu}_t}{\sigma_\epsilon}\frac{\partial}{\partial y}(\tilde{\nu}_t)\right) \\ & + 2\frac{(\sigma_\epsilon - \sigma_k)}{\sigma_k\sigma_\epsilon}\left[\tilde{\nu}_t\frac{\partial^2\tilde{\nu}_t}{\partial y^2} + \left(\frac{\partial\tilde{\nu}_t}{\partial y}\right)^2\right. \\ & \left. + \tilde{\nu}_t^2\frac{1}{\left|\dfrac{\partial u}{\partial y}\right|}\frac{\partial^2}{\partial y^2}\left|\frac{\partial u}{\partial y}\right| + 3\tilde{\nu}_t\frac{\partial\tilde{\nu}_t}{\partial y}\left(\frac{\dfrac{\partial}{\partial y}\left|\dfrac{\partial u}{\partial y}\right|}{\left|\dfrac{\partial u}{\partial y}\right|}\right)\right]\end{aligned} \tag{8}$$

Equation (8) is complicated and difficult to solve numerically. However, the contribution of the terms in the last parenthesis of the equation is proportional to the difference in the diffusive coefficients of the k- and the ϵ-equation. For a number of k-ϵ models these coefficients are equal and the whole term is exactly zero. It was shown in detail in Menter (1994c) that the influence of these terms is small and can be neglected. The second assumption in the derivation of the model is therefore:

$$\sigma_k = \sigma_\epsilon \equiv \sigma \tag{9}$$

The resulting high Reynolds number form of the equation is:

$$\frac{D\tilde{\nu}_t}{Dt} = c_1\tilde{\nu}_t\left|\frac{\partial u}{\partial y}\right| - c_2\frac{\tilde{\nu}_t^2}{L_{VK}^2} + \frac{\partial}{\partial y}\left(\frac{\tilde{\nu}_t}{\sigma}\frac{\partial}{\partial y}(\tilde{\nu}_t)\right) \tag{10}$$

Equation (10) involves the inverse of the von Karman similarity length-scale L_{VK}:

$$\frac{1}{L_{VK}} = \frac{\dfrac{\partial}{\partial y}\left|\dfrac{\partial u}{\partial y}\right|}{\left|\dfrac{\partial u}{\partial y}\right|} \tag{11}$$

The von Karman length-scale was not very successful when used in a mixing length model, mainly because it is singular whenever the denominator goes to zero. In the present one-equation model, the singularity (of the inverse of L_{VK}) is not a problem, because the destruction term that involves L_{VK} can be limited by any other term that has the same dimension, as will be shown later. In the framework of eddy viscosity transport models, the von Karman length scale was also utilized in an unpublished model by Baldwin (1993), and in a model by Durbin et al. (1994), but was never formally derived from the k-ϵ model.

The formalism used in the derivation of Eq. (10) can be applied to transform any two-equation eddy viscosity model to a one-equation model. In the Appendix the transformation for the k-ω model is presented.

The coefficients of the one-equation model follow directly from the k-ϵ model constants:

$$c_1 = (c_{\epsilon 2} - c_{\epsilon 1})\sqrt{c_\mu} = 0.144; \quad \sigma = \sigma_k = 1$$

$$c_2 = \frac{c_1}{\kappa^2} + \frac{1}{\sigma} = 1.86 \tag{12}$$

The standard k-ϵ model constants of $c_{\epsilon 1} = 1.44$, $c_{\epsilon 2} = 1.92$, $c_\mu = 0.09 = a_1^2$ and $\sigma_\kappa = 1.0$ have been used. Note that the transformation leads to $c_2 = 2/\sigma_\epsilon = 1.71$ with $\sigma_\epsilon = 1.17$. Since σ was chosen to be equal to σ_k and not equal to σ_ϵ, the coefficient c_2 had to be slightly recalibrated to match the law of the wall.

The key to the understanding of the one-equation model lies in the comparison of Eqs. (6) and (7). For equilibrium flows the two formulations are equivalent and the one-equation model will be very close in performance to the k-ϵ model. For nonequilibrium adverse pressure gradient flows, Bradshaw's relation, Eq. (6), is better confirmed by experiments than Eq. (7). For these flows the ratio of Production/Dissipation becomes larger than one in the outer region of the boundary layer and the k-ϵ model will give higher shear stresses than the one-equation model. Since the k-ϵ model is well known to overpredict shear stress levels for these flows, it is to be expected that the one-equation model will lead to improved predictions. For flows without shear, Bradshaw's relation, Eq. (6), has no meaning, and the one-equation model cannot be expected to give good results. An example is isotropically decaying turbulence, where one-equation models predict that the eddy viscosity stays constant, whereas the k-ϵ model predicts, more realistically, a decay of the turbulent variables. This deficiency is associated with the lack of a second scale in the model. For shear flows the second scale is provided by the mean shear rate. Regions where the mean shear is locally zero are bridged by the diffusion and the convection terms. Note, however, that the overwhelming

majority of applications of turbulence models is for shear flows, for which one-equation models are well suited.

The main assumption in the derivation of the one-equation model is that the turbulent shear stress is proportional to the turbulent kinetic energy. In standard two equation models this assumption is equivalent to:

$$\text{Production}_k = \text{Dissipation}_k \tag{13}$$

used in the derivation of the Baldwin-Barth model. However, in that model only the production and dissipation terms are transformed based on Eq. (13). The diffusion terms are not transformed exactly. The high Reynolds number form of the Baldwin-Barth (BB) model reads:

$$\frac{D\tilde{\nu}_t}{Dt} = \hat{c}_1\tilde{\nu}_t\left|\frac{\partial u}{\partial y}\right| - \hat{c}_2\frac{\partial\tilde{\nu}_t}{\partial y}\frac{\partial\tilde{\nu}_t}{\partial y} + \frac{\partial}{\partial y}\left(\frac{\tilde{\nu}_t}{\hat{\sigma}}\frac{\partial}{\partial y}(\tilde{\nu}_t)\right) \tag{14}$$

The original Baldwin-Barth model solves an equation for the turbulent Reynolds number. In order to allow a one-to-one comparison of the constants, it has been reformulated here (exactly) as an equation for the eddy viscosity. The transformed constants for this model are:

$$\hat{c}_1 = (c_{\epsilon 2} - c_{\epsilon 1})\sqrt{c_\mu} = 0.24; \quad \hat{\sigma} = \sigma_\epsilon = 0.7$$

$$\hat{c}_2 = \frac{\hat{c}_1}{\kappa^2} + \frac{1}{\hat{\sigma}} = 2.86 \tag{15}$$

They are based on $c_{\epsilon 1} = 1.2$, $c_{\epsilon 2} = 2.0$, $c_\mu = 0.09 = a_1^2$ and $\sigma_\epsilon = 0.7$ for the underlying k-ϵ model. The low Reynolds number form of this model can be found in Baldwin and Barth (1990) and is not repeated here.

In order to distinguish the new model, Eq. (10), from the other models in this study, we call it $(k\text{-}\epsilon)_{1E}$ model where the subscript stands for one-equation. The main difference between the $(k\text{-}\epsilon)_{1E}$ and the BB model is the form of the destruction term (c_2 term). Although the derivation of the BB model starts out from the k-ϵ model, a comparison with Eq. (8) shows that a number of additional assumptions were introduced in order to arrive at Eq. (14). The link between the BB model and the k-ϵ model is thereby broken and it is for this reason that the two models perform very differently, as will be shown later.

Low Reynolds Number Terms. The assumptions leading to the $(k\text{-}\epsilon)_{1E}$ model are obviously not correct in the viscous sublayer, so that the low Reynolds number terms of the k-ϵ model cannot be carried over to the one-equation model. This is not a great loss because the near wall terms of the k-ϵ model are generally complicated and difficult to integrate so that a one-to-one transformation is not desirable.

The purpose of damping functions is to reduce the eddy viscosity in the sublayer. In the present model this is achieved by reducing the production term near the wall and by multiplying the high Reynolds number eddy viscosity, $\tilde{\nu}_t$, by a damping function in order to arrive at the corrected eddy viscosity, ν_t. The damping functions are designed in a pragmatic way that ensures that the resulting model is numerically stable and does not require excessive grid resolution near the surface. Two damping functions are introduced, D_1 in front of the production term and D_2 into the definition of the eddy viscosity:

$$c_1\tilde{\nu}_t\left|\frac{\partial u}{\partial y}\right| \rightarrow D_1 c_1\tilde{\nu}_t\left|\frac{\partial u}{\partial y}\right| \tag{16}$$

$$\nu_t = D_2\tilde{\nu}_t \tag{17}$$

based on the following expressions:

$$D_1 = \frac{\nu_t + \nu}{\tilde{\nu}_t + \nu} \tag{18}$$

$$D_2 = 1 - e^{-(\tilde{\nu}_t/A^+\kappa\nu)^2} \tag{19}$$

and $\kappa = 0.41$. Furthermore, the molecular viscosity is added into the diffusion term in analogy to the k-ϵ model. The coefficient A^+ is equal to $A^+ = 13$.

General Form of the Equations. In order to arrive at an invariant formulation, all occurrences of the strain rate are replaced by the following invariant expression:

$$\left|\frac{\partial u}{\partial y}\right| \rightarrow S = \sqrt{U_{i,j}(U_{i,j} + U_{j,i})} \tag{20}$$

As has been pointed out by Spalart and Allmaras (1994), alternative formulations like the absolute value of the vorticity, or $\sqrt{U_{i,j}U_{i,j}}$ are possible, but for thin shear flows there is little difference among them. In general, applications S has the advantage of being invariant under system rotation and of not producing turbulence under solid body rotation. The term involving the inverse of the von Karman length-scale becomes:

$$E_{k\text{-}\epsilon} \equiv \tilde{\nu}_t^2\left(\frac{1}{L_{VK}}\right)^2 = \tilde{\nu}_t^2\left(\frac{\dfrac{\partial S}{\partial x_j}\dfrac{\partial S}{\partial x_j}}{S^2}\right) \tag{21}$$

An alternative but numerically more expensive (and not yet tested) form would be:

$$E_{k\text{-}\epsilon} = \tilde{\nu}_t^2\left(\frac{1}{L_{VK}}\right)^2 = \tilde{\nu}_t^2\left(\frac{\dfrac{\partial^2 u_i}{\partial x_j\partial x_j}\dfrac{\partial^2 u_i}{\partial x_k\partial x_k}}{\dfrac{\partial u_s}{\partial x_l}\dfrac{\partial u_s}{\partial x_l}}\right) \tag{22}$$

Similarly, all y-derivatives are replaced by their complete invariant forms.

As was pointed out previously, the inverse of the von Karman length-scale can become singular whenever S goes to zero, leading to an infinite destruction term $E_{k\text{-}\epsilon}$. In order to prevent this from happening, the destruction term is limited by a multiple of the Baldwin-Barth destruction term, E_{BB}:

$$E_{1e} = c_3 E_{\text{BB}} \tanh\left(\frac{E_{k\text{-}\epsilon}}{c_3 E_{\text{BB}}}\right) \tag{23}$$

with a constant $c_3 = 7$. E_{BB} is defined as:

$$E_{\text{BB}} = \frac{\partial\tilde{\nu}_t}{\partial x_j}\cdot\frac{\partial\tilde{\nu}_t}{\partial x_j} \tag{24}$$

Equation (23) provides a smooth transition between the two formulations whenever $E_{k\text{-}\epsilon}$ goes to infinity. For most of the flow $E_{k\text{-}\epsilon} \ll c_3 E_{\text{BB}}$ and the original formulation is recovered. A less smooth transition could be achieved by $E_{1e} = \min(E_{k\text{-}\epsilon}; c_3 E_{\text{BB}})$. The numerical results are not sensitive to the constant c_3.

The final form of the $(k\text{-}\epsilon)_{1E}$ model is:

$$\frac{D\tilde{\nu}_t}{Dt} = c_1 D_1\tilde{\nu}_t S - c_2 E_{1e} + \frac{\partial}{\partial x_j}\left(\left(\nu + \frac{\tilde{\nu}_t}{\sigma}\right)\frac{\partial}{\partial x_j}(\tilde{\nu}_t)\right) \tag{25}$$

$$\nu_t = D_2\tilde{\nu}_t \tag{26}$$

Note that the above equations are still strictly local, without dependence on the distance from the surface.

Numerical Results

Free Shear Flows. Self-similar shear layers are very important test cases which provide insight into the performance of turbulence models, without the need for large computer resources. In this section, the models will be tested against the standard free shear cases, namely, a self-similar mixing layer,

Table 1 Definition of variables for free shear flows

Far wake	Mixing layer	Plane/round jet	
U	$u(x, y) = U_\infty - \sqrt{\frac{D}{\rho x}}\, U(\eta)$	$u(x, y) = U_1 U(\eta)$	$u(x, y) = \frac{J}{x^{(j+1)/2}}\, U(\eta)$
N	$v_t(x, y) = \frac{D}{\rho U_\infty} N(\eta)$	$v_t(x, y) = x U_1 N(\eta)$	$v_t(x, y) = \sqrt{J} x^{(1-j)/2} N(\eta)$
η	$\eta = y\sqrt{\frac{\rho U_\infty^2}{Dx}}$	$\eta = \frac{y}{x}$	$\eta = \frac{y}{x}$
Additional definitions	$D = 2\int_0^\infty \rho u(U_\infty - u)dy$	—	$J = \frac{\pi_j}{2}\int_0^\infty u^2 y^j dy$

the plane and round jet and the self similar far wake. The equations are cast into self-similar form following Wilcox (1993), resulting in the following two ordinary differential equations for the nondimensional velocity U and the nondimensional eddy viscosity N:

$$V\frac{dU}{d\eta} - \frac{1}{\eta^j}\frac{d}{d\eta}\left[\eta^j N\frac{dU}{d\eta}\right] = S_U U \tag{27}$$

$$V\frac{dN}{d\eta} - \frac{1}{\eta^j}\frac{d}{d\eta}\left[\frac{1}{\sigma}\eta^j N\frac{dN}{d\eta}\right] = S_N N + c_1\left|\frac{dU}{d\eta}\right| - c_2\left(\frac{N}{L_{VK}}\right)^2 \tag{28}$$

with:

$$\frac{1}{L_{VK}} = \frac{\frac{1}{\eta^j}\frac{d}{d\eta}\left(\eta^j\left|\frac{dU}{d\eta}\right|\right)}{\left|\frac{dU}{d\eta}\right|} \tag{29}$$

where $j = 1$ for the round jet and $j = 0$ for the plane flows. The nondimensional variables are defined as given in Table 2 and Table 3: The coefficients in Table 2 can be obtained from Wilcox (1993) and $S_N = 2S_K - S_\epsilon$. (Note that the coefficient S_K in Wilcox (1993) should be $2U$ for the round jet.)

Asymptotic Solution Near Shear Layer Edge for the (k-ϵ)$_{1E}$ and the Baldwin-Barth Model. The analysis of the asymptotic solution near the edge of turbulent layer is an important part of turbulence model evaluation. It is especially important to determine the sensitivity of the solution to changes in the freestream values specified for the turbulence variables outside the layer. Models with solutions that change significantly with the freestream conditions are not acceptable, because the "correct" freestream conditions are not known in most applications. The problem has been analyzed in detail by Menter (1992a) and Cazalbou et al. (1994) for two-equation eddy viscosity models. It was shown that the k-ω model has a severe dependency on the values specified for ω outside the layer. It was also shown that the k-ϵ model does not suffer from this ambiguity. There is no theory available to decide whether a model has a freestream sensitivity, but the existence of an asymptotic algebraic solution near the boundary layer edge seems to be at least a necessary condition for a model to be well conditioned.

The analysis does not depend on which shear flow is selected for the analysis, since the existence of an algebraic solution implies that the terms involving S_U and S_N decay faster than the other terms near the edge of the layer and can therefore be neglected. The new variable $\tilde{\eta} = \eta - \delta$ is introduced near the shear layer edge, δ, and algebraic solutions of the form:

$$\frac{dU(\eta)}{d\tilde{\eta}} = A\tilde{\eta}^\alpha; \quad N(\tilde{\eta}) = B\tilde{\eta}^\beta \tag{30}$$

are introduced into the equations. Straightforward algebra shows that the exponents for the (k-ϵ)$_{1E}$ model are:

$$\alpha = \frac{\left(-1 + \sqrt{1 - 4c_2\left(1 - \frac{1}{\sigma}\right)}\right)}{2c_2} = 0; \quad \beta = 1 \tag{31}$$

Therefore, the velocity and the eddy viscosity approach the shear layer edge linearly. It is interesting to note that the solution for the k-ϵ model is also linear for $\sigma_k = \sigma_\epsilon = 1$ so that the asymptotic behavior of the k-ϵ model carries over to the present one-equation model.

The Baldwin-Barth model does not have a solution of the form given by Eq. (30). However, as pointed out before, there is no theory available to show that the existence of algebraic solutions is a sufficient, or even a necessary condition to prevent free stream dependency. Numerical test will have to be used to obtain insight into the model characteristics.

Figure 1 shows spreading rates for a far wake, computed with the Baldwin-Barth model as a function of the freestream value, N_f, and the number of grid points, n, across the layer $0 \le \eta \le 0.4$. The gridpoints are evenly distributed and the highest freestream values shown in Fig. 1 are 2 percent of the maximum value of N inside the layer. The Baldwin-Barth model shows a

Table 2 Coefficients for free shear flows

Flow	S_U	S_N	$V(\eta)$
Far wake	1/2	0	$-\frac{1}{2}\eta$
Mixing layer	0	$-U$	$-\int_0^\eta U(\eta')d\eta'$
Plane jet	1/2U	$-1/2U$	$-\frac{1}{2}\int_0^\eta U(\eta')d\eta'$
Round jet	U	0	$-\frac{1}{\eta}\int_0^\eta U(\eta')\eta' d\eta'$

Table 3 Spreading rates for free shear flows

Flow	k-ϵ	(k-ϵ)$_{1E}$	Experiment
Far wake	0.256	0.250	0.365
Mixing layer	0.100	0.084	0.115
Plane jet	0.109	0.111	0.100–0.110
Round jet	0.120	0.131	0.086–0.095

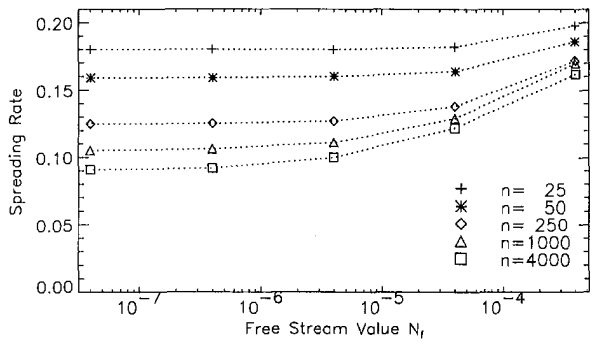

Fig. 1 Spreading rates of the Baldwin-Barth model for far wake, depending on freestream values, N_f, and number of gridpoints, n

strong sensitivity to the values specified for N_f, especially as the grid is refined. Furthermore, none of the solutions is in acceptable agreement with the experimental spreading rate of 0.365 as quoted from Wilcox (1993).

Figure 2 shows the computed velocity profiles on the finest grid (n = 4000) for the highest and the lowest freestream values. It is apparent that the model develops extremely high gradients in the velocity profile for the lower freestream values. The high gradients are the reason why the freestream sensitivity does not show up on the coarse grids, where they cannot be resolved. No grid independent solution could be obtained for the low values of N_f. Even if the number of points is doubled again to n = 8000, the solution develops even higher slopes and lower spreading rates. As with the k-ω model, the influence of the freestream conditions is not restricted to the vicinity of the boundary layer edge, but affects the whole layer. However, the k-ω model becomes more diffusive with decreasing freestream values and no grid sensitivity is observed.

Spalart and Allmaras (1994) have investigated the behavior of a turbulent front and found that for the Baldwin-Barth model the front propagates in the (physically) incorrect direction away from the non-turbulent region. They also report that their results are dependent on the freestream values specified for the eddy viscosity, consistent with the present findings. Spalart (1994) also reports similar problems with the Baldwin-Barth model as shown in Fig. 1 for his computation of a self-similar mixing layer. Like in the present calculations, his results are highly sensitive to grid resolution and free-stream values. On the other hand, Baldwin and Barth (1990) have tested the model for a flat plate zero pressure gradient boundary layer (based on a Navier-Stokes code) and found only a moderate dependency on the freestream values. Note, however, that Navier-Stokes grids are generally coarse near the boundary layer edge (assuming that all points are plotted in Baldwin and Barth (1990), there are about forty points across the boundary layer but only ten of them in the wake region) so that it is apparent that the problem was not resolved in that computation. Note also that the present author has tested the Baldwin-Barth model in Navier-Stokes codes (Menter, 1992b) and did at first not realize the severity of the problem for the same reason. However, Rogers (1994) reported that he could not obtain grid independent solutions for airfoil flows with the Baldwin-Barth model using the INS2D Navier-Stokes code.

Goldberg et al. (1994) and Goldberg (1994) have proposed a number of "pointwise" one-equation models, which are, in their high Reynolds number version, formally identical to the Baldwin-Barth model (note that the present problems are independent of the low Reynolds number treatment). Although Goldberg does not report problems near the edge of turbulent layers, computations by the present author have shown the same deficiencies as with the BB model. Furthermore, the results presented in Goldberg (1994) for self-similar flows could not be reproduced with any reasonable combination of freestream values and grid distributions. These references are therefore not considered in the present discussion.

What are the implications of the results shown in Figs. 1–2 for Navier-Stokes applications? There are two different strategies. The first one is to specify small values for the eddy viscosity in the freestream (inflow). The advantage of low values is that they can be specified unambiguously—values that are a fraction of the molecular viscosity will ensure that they are small compared to those inside the layer. However, due to the large gradients developing in this case, no grid independent solutions can be obtained, a situation not acceptable in a Navier-Stokes code. The second strategy is to specify large freestream values (say x percent of the maximum values inside the layer). Tests have shown that in order to reproduce the experimental spreading rates of free shear flows, freestream values of about 20–30 percent of the maximum inside the layer have to be used. Values that high would severely impact laminar regions in the flowfield and are certainly not acceptable.

The $(k$-$\epsilon)_{1E}$ model was subjected to the same tests as the Baldwin-Barth model. The model did not show any freestream dependency, as long as the freestream values are small (<1 percent) compared to the values inside the layer. Furthermore the solution for the $(k$-$\epsilon)_{1E}$ model did follow the algebraic solution given by Eq. (30) near the boundary layer edge. Even for very small values, grid independent solutions were obtained with only about 15 points inside the half-layer.

Table 3 compares the spreading rates of free shear layers as computed with the standard k-ϵ and the $(k$-$\epsilon)_{1E}$ model. The experimental values are taken from Wilcox (1993). The Baldwin-Barth model is not included because no grid- or freestream independent solutions could be obtained. It is interesting to note that the $(k$-$\epsilon)_{1E}$ model gives very similar spreading rates to the k-ϵ despite the fact that Bradshaw's assumption is not generally true for these flows.

Self-Similar Boundary Layer Flows. Wilcox (1993) has popularized the use of defect layer computations for testing turbulence models under equilibrium pressure gradient conditions. As expected, the Baldwin-Barth model has the same freestream dependency as for the free shear layers. Figure 3 shows computations with this model for the zero pressure gradient boundary layer experiment of Wieghardt (Kline et al., 1981) with two different freestream values on a fine grid of 1000 points. The high freestream value is about 1 percent of the maximum eddy viscosity value inside the boundary layer. Again, the solution develops extreme gradients near the boundary layer edge for the low freestream values. The same computations have shown only a moderate sensitivity on a coarse grid.

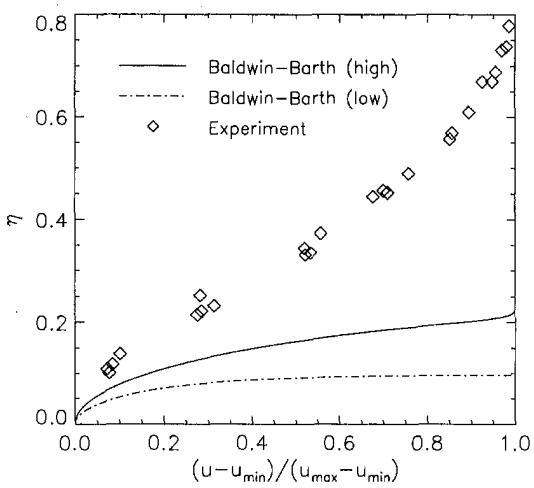

Fig. 2 Velocity profiles for far wake with Baldwin-Barth model for highest and lowest freestream values (number of gridpoints, n = 4000.)

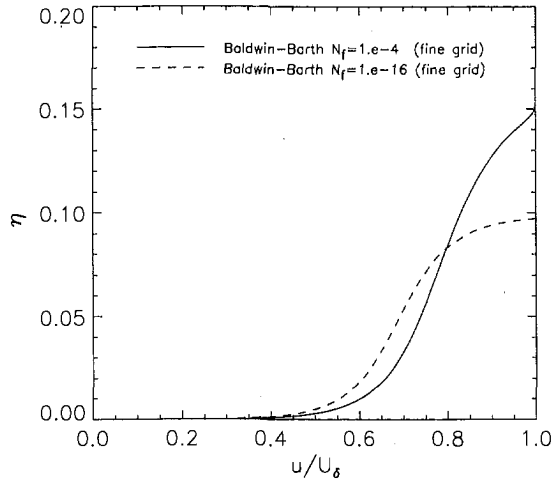

Fig. 3 Velocity profiles for defect layer with Baldwin-Barth model and two different freestream values, N_f, (fine grid with n = 1000)

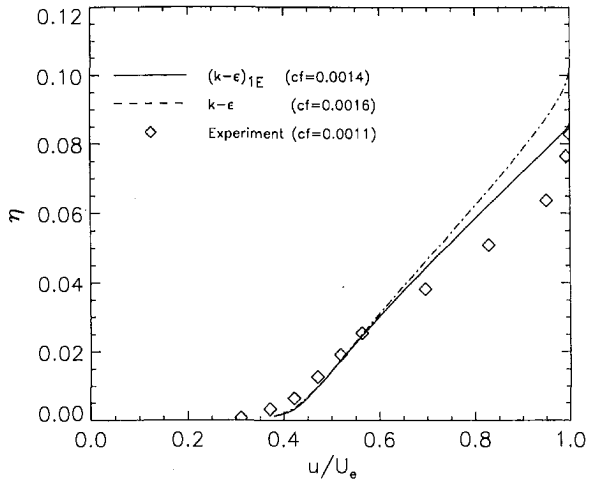

Fig. 5 Velocity profiles for defect layer, β_T = 8.7

It is obvious from these results that the freestream sensitivity could not be resolved in Baldwin and Barth (1990). As in the free shear layer computations, the influence of the freestream values and grid densities is not confined to the vicinity of the boundary layer edge, but affects the whole layer. No grid converged solution could be obtained with the Baldwin-Barth model for the low freestream value. From the present study it is not clear whether an asymptotic solution exists for this model as N_f goes to zero and the number of grid points goes to infinity. Whenever the number of grid-points was increased, the solution changed with an increase in the slope near the edge and a lower eddy viscosity inside the layer.

Figure 4 shows a comparison of results for the zero pressure gradient case of Wieghardt for the k-ϵ and the $(k$-$\epsilon)_{1E}$ models. Both models give very accurate velocity profiles and c_f-predictions.

Figure 5 shows the velocity profiles for the adverse pressure gradient flow of Clauser (Kline et al., 1981) for a nondimensional pressure gradient of β_T = 8.7. It is well known that the standard k-ϵ model overpredicts the skin friction for adverse pressure gradient flows, in this case by about 50 percent. Note that the apparent differences in boundary layer thickness between the computations and the experiment are a result of the definition of η, involving the friction velocity u_τ. The introduction of Bradshaw's relation, Eq. (6), into the $(k$-$\epsilon)_{1E}$ model obviously improves the predictions, but the skin friction is still too high by about 30 percent. Due to the close relationship of the $(k$-$\epsilon)_{1E}$ model to the standard k-ϵ model, it had to be expected that the deficiency in the adverse pressure gradient behavior of the k-ϵ model would not entirely be avoided by the new model.

Navier-Stokes Computations. All of the following test cases have been computed with the NASA Ames INS2D and INS3D codes (Rogers and Kwak, 1988). All flows in this study are part of a test base assembled by the author to evaluate the performance of turbulence models. The flows have been set up in a way to match the experimental boundary conditions as closely as possible. Furthermore, all computations are performed on grids that have been shown to produce grid independent solutions. A number of additional test of the present models can be found in Menter (1994c). All k-ϵ model computations were based on Launder and Sharma (1974).

It was initially intended to compare results of all three models for the following Navier-Stokes applications. However, due to the severe deficiencies discovered in the Baldwin-Barth model for the equilibrium flows, the model was dropped from the study since the results are invariably either grid- or freestream dependent.

Flat Plate Zero Pressure Gradient Boundary Layer. Figure 6 shows a comparison of the computed wall skin friction coefficients, c_f, versus displacement thickness, θ, for a flat plate zero pressure gradient boundary layer. The computations are

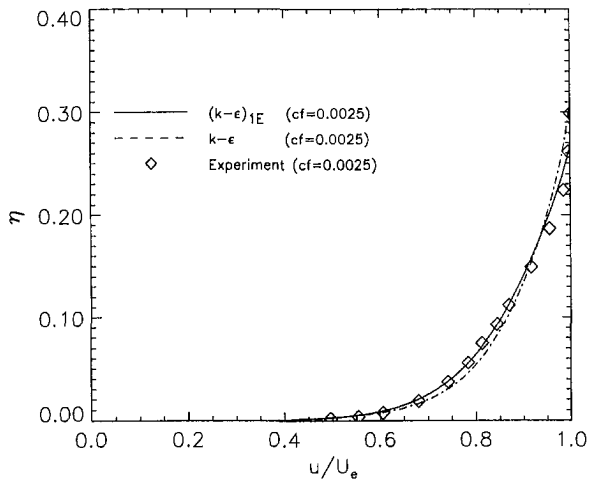

Fig. 4 Velocity profiles for defect layer, β_T = 0

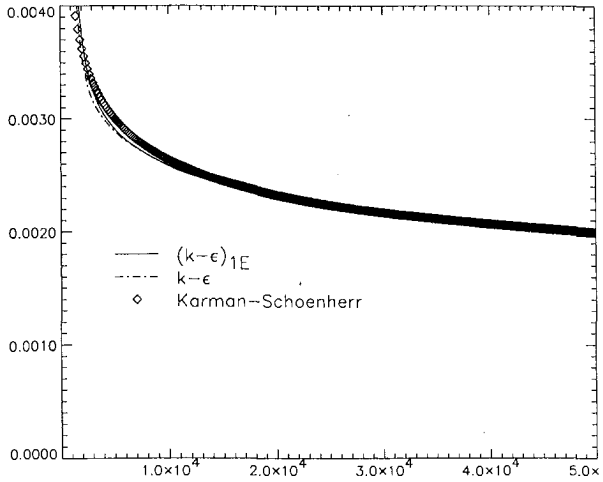

Fig. 6 Skin-friction coefficient for flat plate boundary layer

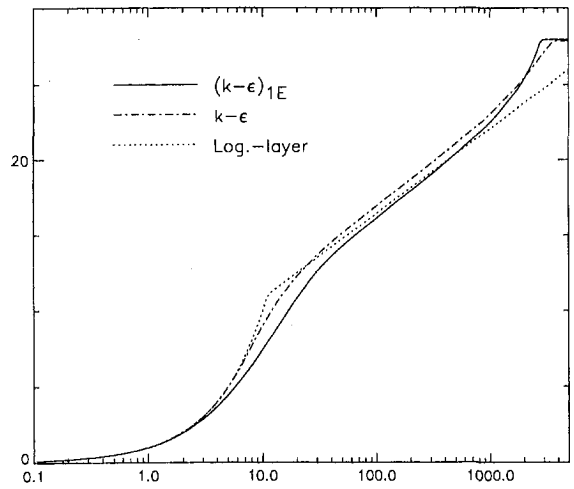

Fig. 7 Velocity profiles for flat plate boundary layer in inner coordinates

compared with the experimental correlation of v. Karman and Schoenherr. The low Reynolds number version of the k-ϵ model is due to Launder and Sharma (1974). Both models are in good agreement with the experimental correlation. The one-equation model gives accurate results, as long as the first grid point satisfies $y_1^+ < \sim 2.0$. The Launder-Sharma model requires a significantly smaller grid-spacing near the wall of $y_1^+ < \sim 0.3$. (Note that a finer grid-spacing is used compared to Menter (1994c), leading to improved results for the Launder-Sharma model.)

The velocity profiles in inner coordinates are depicted in Fig. 7. Again both models are in good agreement with the law of the wall.

Driver Separated Adverse Pressure Gradient Flow. In Driver's flow (Driver, 1991), a turbulent boundary layer develops in the axial direction of a circular cylinder. A strong adverse pressure gradient is imposed on the flow by diverging wind tunnel walls plus suction applied at these walls. The pressure gradient is strong enough to cause the flowfield to separate. The inflow Reynolds number is 2.8×10^5 based on the diameter, D, of the cylinder. The inflow boundary layer thickness is about $0.2D$. The experiments offer independent wall-skin friction measurements and it was found in previous tests (Menter, 1994c) that the data are highly self-consistent and well suited to test models under strong pressure gradient conditions. The computations are performed on a $60 \times 3 \times 60$ (verified on a $90 \times 3 \times 90$) grid.

Figure 8 shows the wall skin friction coefficient for this flow. As in previous comparisons, the standard k-ϵ model predicts

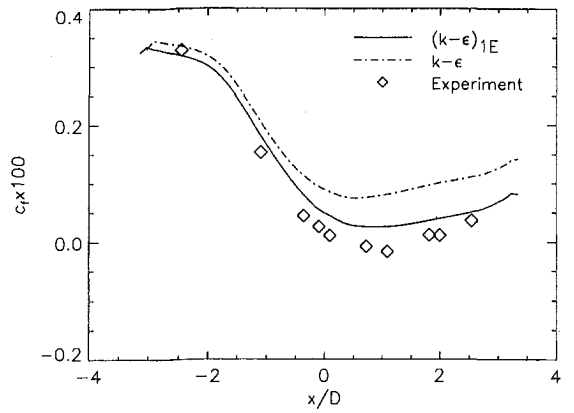

Fig. 8 Skin-friction for Driver's case CS0

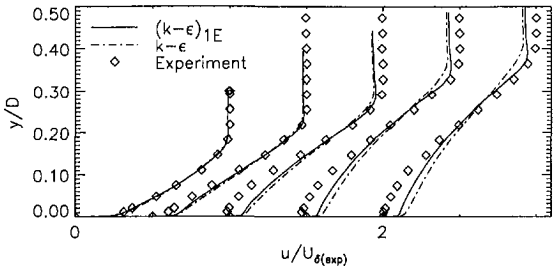

Fig. 9 Velocity profiles for Driver's case CS0 at x/D = −0.544, −0.091, 0.363, 1.088, 1.633

significantly higher values than the experiment. The $(k$-$\epsilon)_{1E}$ model is in better agreement with the data, but still somewhat too high, especially in the region where the experiment shows separation.

For the velocity profiles shown in Fig. 9 the one-equation model is a little closer to the data, but both models underpredict the viscous-inviscid interaction. Again, the $(k$-$\epsilon)_{1E}$ model predicts a stronger retardation due to the pressure gradient, but not enough to be in good agreement with the data.

As the flow encounters more severe nonequilibrium conditions, the differences between Bradshaw's relation, Eq. (6), and the relation enforced by the two-equation model, Eq. (7), become more severe and the predictions of the two models start to deviate. Figure 10 shows the ratio of production versus dissipation as predicted by the standard k-ϵ model at the location of the maximum turbulent shear stress. This ratio is an indicator of the nonequilibrium effects and enters into Eq. (7). Since Bradshaw's relation is generally more realistic than Eq. (7), the $(k$-$\epsilon)_{1E}$ model gives better results than the standard k-ϵ model.

Backward Facing Step Flow. The backward facing step is one of the most widely used test cases for turbulence model evaluation. While early results for this flow indicated that the k-ϵ model underpredicts the reattachment length by ~30 percent, more recent results have shown that the model is off by only about 5 percent. The earlier computations had not enough resolution to accurately predict the flow. The test case in this study is the flow of Driver and Seegmiller (1985). The Reynolds number, based on the upstream momentum thickness Θ is Re_Θ = 5,000 and the ratio of the boundary layer thickness to step height is about 1.5. The expansion ratio is 1.125. The computations have been performed on a 120×120 grid with substantial grid refinement near the step. The computations are virtually identical to those performed on a 240×240 grid.

Figure 11 shows the computed and the experimental skin friction distributions. The k-ϵ model underpredicts the reattachment location by about 5 percent and is generally not in good agreement with the data in the separated region and

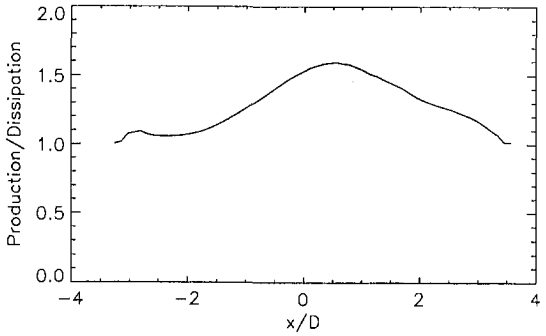

Fig. 10 Ratio of Production/Dissipation for Driver's case CS0 as computed from the k-ϵ model

near reattachment. Different low Reynolds number forms of this model give different skin friction distribution, so that this behavior is certainly a result of the low-Reynolds number terms. The $(k\text{-}\epsilon)_{1E}$ model is in very good agreement with the data. The reattachment location is predicted within experimental uncertainty, and there are no overshoots near reattachment. Especially impressive is the skin friction recovery downstream of reattachment, where other models tend to fall more severely below the experiments (Menter, 1994a; Menter, 1993; Menter, 1994c).

The velocity profiles depicted in Fig. 12 show that the high Reynolds number differences between the models are amazingly small. The velocity profiles are almost identical even inside the separation bubble and it appears again that the two-equation model does not offer an advantage over the one-equation model. Both of the present models fail to predict the recovery of the velocity profiles downstream of reattachment. This is a general problem with existing models and has been observed before (Menter, 1994c).

Conclusions

The connection between one- and two-equation models of turbulence has been reexamined. It was found that the standard k-ϵ model can be transformed into a one-equation model based on only two assumptions. The first assumption is Bradshaw's relation that the turbulent shear stress is proportional to the turbulent kinetic energy. This assumption corresponds to $\text{Production}_k = \text{Dissipation}_k$ in standard two equation models and is therefore closely satisfied for equilibrium flows. For nonequilibrium flows, Bradshaw's relation is actually better confirmed by experiments than the relation enforced by the standard k-ϵ model. The second assumption is that the diffusion coefficients in the k- and the ϵ-equations are identical. By enforcing this condition in the k-ϵ model, it was shown in Menter (1994c) that only minor changes resulted from it. The new model was termed $(k\text{-}\epsilon)_{1E}$ model and tested against the Baldwin-Barth model and the standard k-ϵ model.

Free-shear layer computations have shown that the Baldwin-Barth model is ill-conditioned near the boundary layer edge. The model does not posses an algebraic solution in that region and produces unlimited gradients in the velocity as the grid is refined. Furthermore, results are sensitive to the freestream values specified outside the layer. No grid and freestream independent results could be obtained with this model and it was for this reason not included in the rest of the study. The reason for the failure of the model lies in a destruction term that does not follow from the transformation of the two-equation model.

The findings for the Baldwin-Barth model re-emphasize that the behavior of turbulence models near the turbulent-nonturbulent interface is one of the most important aspects of turbulence modeling. Shortcomings in that area are not confined to the immediate vicinity of the interface, but change the solution through the whole layer, essentially nullifying the calibration process. Unfortunately, not enough attention is paid to this problem in the derivation and calibration of most new models, leaving the door open for potentially devastating failures. This is also true for Reynolds stress models.

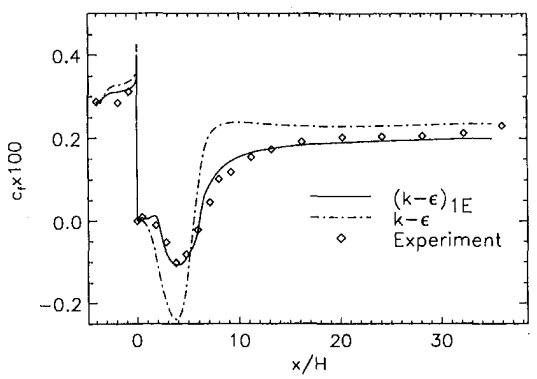

Fig. 11 Skin-friction for backward facing step flow

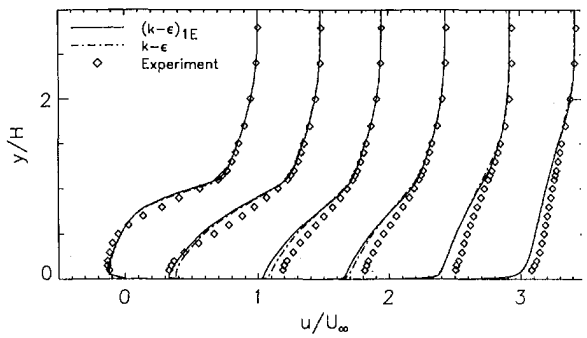

Fig. 12 Velocity profiles for backward facing step flow at x/h = 2, 4, 6.5, 8, 14, 32

The new one-equation model does not suffer from these deficiencies and shows a very close similarity to its parent two-equation model near the boundary layer edge. A comparison of the free shear layer results has shown that the predictions of the one- and two-equation models are fairly close to one another.

The one-equation model gives almost identical results to the k-ϵ model for zero pressure gradient boundary layers. A number of increasingly stronger adverse pressure gradient flows has shown that the results of the one-equation model improve compared to the k-ϵ model predictions as the nonequilibrium effects become more important. The improved results confirm that the main assumption going into the $(k\text{-}\epsilon)_{1E}$ model is more realistic than the relation enforced by the k-ϵ model.

The computations have shown that the new one-equation model produced very similar, and for boundary layer flows improved results when compared to the standard k-ϵ model. Because of its simplicity, the model is also attractive from a computational standpoint. However, a note of caution should be made concerning the use of the second derivative of the velocity field in the von Karman length scale. From the limited tests the model has undergone at this stage, it is not certain whether the von Karman length scale will be general enough for the computation of complex three-dimensional flow fields, especially for cases that are severely out of equilibrium. Further tests will have to be conducted to evaluate the model under these conditions.

Acknowledgment

This paper has greatly benefited from many important comments by Barrett Baldwin, Peter Bradshaw, Tom Coakley, George Huang, and Philippe Spalart. The research was funded by the NASA Ames Research Center.

APPENDIX

Transforming the k-ω Model

The transformation leading to the $(k\text{-}\epsilon)_{1E}$ can be used to transform any two-equation model into a one-equation model. An example is the k-ω model of Wilcox (1993):

$$\frac{Dk}{Dt} = \nu_t\left(\frac{\partial u}{\partial y}\right)^2 - \beta^* k\omega + \frac{\partial}{\partial y}\left(\sigma\nu_t \frac{\partial}{\partial y}(k)\right)$$

$$\frac{D\omega}{Dt} = \alpha\left(\frac{\partial u}{\partial y}\right)^2 - \beta\omega^2 + \frac{\partial}{\partial y}\left(\sigma\nu_t \frac{\partial}{\partial y}(\omega)\right)$$

In the k-ω model the definition of the eddy viscosity is:

$$\nu_t = \frac{k}{\omega}$$

With the help of Eqs. (3) and (6) the following one-equation model can be derived (high Reynolds number form):

$$\frac{D\tilde{\nu}_t}{Dt} = c_1\tilde{\nu}_t\left|\frac{\partial u}{\partial y}\right| + c_2\tilde{\nu}_t\frac{\dfrac{\partial}{\partial y}\left|\dfrac{\partial u}{\partial y}\right|}{\left|\dfrac{\partial u}{\partial y}\right|}\frac{\partial\tilde{\nu}_t}{\partial y} + \frac{\partial}{\partial y}\left(\sigma\tilde{\nu}_t\frac{\partial}{\partial y}(\tilde{\nu}_t)\right)$$

The constants in this model follow directly from the k-ω constants:

$$c_1 = \frac{\beta}{a_1} - a_1\alpha = 0.0833; \quad c_2 = 2\sigma = 1$$

with:

$$\alpha = \tfrac{5}{9}; \quad \beta = 0.075; \quad \sigma = 0.5; \quad \beta^* = a_1^2 = 0.09$$

Note that the diffusion coefficients in the k- and the ω-equation are equal so that no terms proportional to the difference of these two constants appears (see Eq. (8)).

First tests with this model have shown that the solutions develope large gradients in the velocities near the boundary layer edge, similar to the Baldwin-Barth model. This is possibly due to the small diffusion coefficient of $\sigma = 0.5$. Note also that the k-ω model has a strong dependency on freestream values (Menter, 1992a), which seems to carry over to the one-equation model. More analysis and careful testing, as well as a possible recalibration of the coefficients will be required before the model can be applied to engineering flows.

References

Baldwin, B. S., 1993, personal communication.

Baldwin, B. S., and Barth, T. J., 1990, "A One-Equation Turbulence Model for High Reynolds Number Wall Bounded Flows," NASA TM-102847.

Baldwin, B. S., and Lomax, H., 1978, "Thin Layer Approximation and Algebraic Model for Separated Turbulent Flows," AIAA Paper 78-0257, Huntsville, Ala.

Bradshaw, P., Ferriss, D. H., and Atwell, N. P., 1967, "Calculation of Boundary Layer Development Using the Turbulent Energy Equation," *Journal of Fluid Mechanics,* Vol. 23, pp. 31–64.

Cazalbou, J. B., Spalart, P. R., and Bradshaw, P., 1994, "On the Behavior of Two-Equation Models at the Edge of a Turbulent Region," *Physics of Fluids,* Vol. 6(5), May.

Driver, D. M., 1991, "Reynolds Shear Stress Measurements in a Separated Boundary Layer," AIAA Paper 91-1787.

Driver, D. M., and Seegmiller, H. L., 1985, "Features of a Reattaching Turbulent Shear Layer in Divergent Channel Flows," *AIAA Journal,* Vol. 23, No. 2.

Durbin, P. A., Mansour, N. N., and Yang, Z., 1994, "Eddy Viscosity Transport Model for Turbulent Flow," *Physics of Fluids,* Vol. 6, No. 20, Feb.

Goldberg, U. C., and Ramakrishnan, S. V., 1994, "A Pointwise Version of the Baldwin-Barth Turbulence Model," *International Journal of Computational Fluid Dynamics 1,* No. 4, pp. 321–338.

Goldberg, U. C., 1994, "A Pointwise One-Equation Turbulence Model for Wall-Bounded and Free Shear Flows," *International Symposium on Turbulence, Heat and Mass Transfer,* Lisbon, pp. 13.2.1–13.2.6.

Gulyaev, A. N., Kozlov, V. Y., and Secundov, A. N., 1993, "Universal Turbulence Model "$\nu_t - 92$." Ecolen Report, Moscow.

Johnson, D. A., and King, L. S., 1985, "A Mathematically Simple Closure Model for Attached and Separated Turbulent Boundary Layers," *AIAA Journal,* Vol. 23, Nov., pp. 1684–1692.

Kline, S. J., Cantwell, B. J., Lilley, G. M., 1981, eds., "1980–1981 AFOSR-HTTM Stanford Conference on Complex Turbulent Flows," Comparison of Computation and Experiment, Stanford University, Stanford, CA.

Launder, B. E., and Sharma, B. I., 1974, "Application of the Energy Dissipation Model of Turbulence to the Calculation of the Flow Near a Spinning Disc," *Letters in Heat and Mass Transfer,* Vol. 1, No. 2, pp. 131–138.

Menter, F. R., 1992a, "Influence of Freestream Values on k-w Turbulence Model Predictions," *AIAA Journal,* Vol. 30, No. 6.

Menter, F. R., 1992b, "Performance of Popular Turbulence Models for Attached and Separated Adverse Pressure Gradient Flows," *AIAA Journal,* Vol. 30, No. 8, Aug., pp. 2066–2072.

Menter, F. R., 1993, "Zonal Two Equation k-w Turbulence Models for Aerodynamic Flows," AIAA Paper 93-2906, Orlando, FL.

Menter, F. R., 1994a, "A Critical Evaluation of Promising Eddy-Viscosity Turbulence Models," *Proceedings Intern. Symp. on Turbulence, Heat and Mass Transfer,* Portugal, pp. 13.4.1–13.4.6.

Menter, F. R., 1994b, "Two-Equation Eddy-Viscosity Turbulence Models for Engineering Applications," *AIAA Journal,* Vol. 32, No. 8, pp. 1598–1605.

Menter, F. R., 1994c, "Eddy Viscosity Transport Equations and there Relation to the k-ϵ Model," NASA TM 108854.

Menter, F. R., and Rumsey, C. L., 1994, "Assessment of Two-Equation Models for Transonic Flows," AIAA Paper 94-2343, Colorado Springs, CO.

Nee, V. W., and Kovasznay, L. S. G., 1969, "Simple Phenomenological Theory of Turbulent Shear Flows," *The Physics of Fluids,* Vol. 12, No. 3, Mar., pp. 473–484.

Rogers, S. E., 1994, personal communication.

Rogers, S. E., and Kwak, D., 1988, "An Upwind Differencing Scheme for the Time-Accurate Incompressible Navier-Stokes Equations," AIAA Paper 88-2583, Williamsburg, Va.

Samuel, A. E., and Joubert, P. N., 1974, "A Boundary Layer Developing in an Increasingly Adverse Pressure Gradient," *Journal of Fluid Mechanics,* Vol. 66, Part 3, pp. 481–505.

Spalart, P. R., 1994, personal communication.

Spalart, P. R., and Allmaras, S. R., 1994, "A One-Equation Turbulence Model for Aerodynamic Flows," *La Recherche Aerospatiale,* No. 1, pp. 5–21.

Townsend, A. A., 1962, "Equilibrium Layers and Wall Turbulence," *Journal of Fluid Mechanics,* Vol. 11.

Wilcox, D. C., 1993, *Turbulence Modeling for CFD,* DCW Industries, Inc., La Canada, CA.